

**Self-completed Joule heat welding of ultrathin Pt wires**

Hironori Tohmyoh\* and Satoru Fukui

*Department of Nanomechanics, Tohoku University, Aoba 6-6-01, Aramaki, Aoba-ku, Sendai 980-8579, Japan*

(Received 13 June 2009; revised manuscript received 5 September 2009; published 2 October 2009)

Two Pt wires with diameters of about 800 nm were successfully welded by Joule heating in a scanning electron microscope. Melting and solidification at the point contact of the thin wires occurred continuously under a constant current supply and the welding process was completed within several seconds. This rapid and self-completed welding is due to the geometrical features of the nanocontact and the heat transport properties of the thin wires. The current required for joining wires in a scanning electron microscope was much lower than that in air. This is remarkable for longer wires and was found to be due to greater insulation under high-vacuum conditions. The difference in the thermal boundary conditions, in other words the difference in the melting conditions at the nanocontact, was evaluated experimentally and a parameter, comprising the applied current, the geometrical quantities of the wires, and a function for calibrating the thermal boundary conditions, with which the conditions for welding thin wires under different vacuum levels could be determined, is presented.

DOI: [10.1103/PhysRevB.80.155403](https://doi.org/10.1103/PhysRevB.80.155403)

PACS number(s): 81.20.Vj, 81.07.Lk, 81.16.Dn, 44.90.+c

**I. INTRODUCTION**

The importance of cutting and welding technologies for low-dimensional materials, e.g., metallic or semiconductor nanowires (NWs),<sup>1-6</sup> carbon nanotubes (CNTs),<sup>7-12</sup> polymer nanofibers,<sup>13</sup> and nanoparticles,<sup>14</sup> has been increasing day by day because these technologies are indispensable for modifying these materials for specific purposes or assembling them in systems in many fields of application. Moreover, welding technologies for low-dimensional materials have been found to be effective for manipulating materials<sup>11</sup> and for generating functional elements, e.g., thermoelectric<sup>15,16</sup> and optical elements,<sup>17</sup> etc.

Techniques that use an electron beam<sup>2,3,9,11</sup> or laser beam<sup>14</sup> can provide local noncontact heating of small-scale materials and these are capable of welding two objects at a specified point without problems arising from the geometry of the objects. These techniques, however, are difficult to apply at shadow points that are obscured from the electron or laser beam. In contrast with the above-mentioned techniques, cutting and welding techniques for conductive materials utilizing Joule heating can be used for a wide range of applications because heat can easily be induced by a current supply.<sup>5,6,8,12</sup> A metal particle<sup>12</sup> and a metal nanovolume solder<sup>6</sup> have recently been found to be effective for Joule heat welding of low-dimensional materials.

Welding is accomplished by phase transition of the material at the contact point. First, melting at the point of contact occurs and then the molten part solidifies. Low-dimensional materials show unusual thermal behavior due to their specific geometry and properties.<sup>18</sup> Moreover, the melting point of low-dimensional materials is found to be lower than their bulk equivalents.<sup>19-21</sup> Consequently, controlling the melting and solidification phenomena for low-dimensional materials is not an easy task. Very recently, a parameter that governs the melting phenomenon at the nanocontact of two thin wires in air was presented.<sup>22</sup>

In this paper, we report on Joule heat welding of thin Pt wires performed in a scanning electron microscope (SEM)

and in air and discuss the difference in welding conditions due to the difference in the environmental conditions, i.e., the vacuum level. Thin Pt wires with diameters of about 800 nm were successfully welded in both an SEM and in air, but the currents required for welding were remarkably different in each environment. The difference in the conditions for successful welding was found to be due to the difference in heat transfer from the wire surface to the environment and this can be accurately described by a thermal function. The welding conditions for two wires can be determined by a parameter that includes the thermal function. The welding process was continuously recorded together with the circuit voltage history. From *in situ* monitoring of the welding process, it was found that melting and solidification at the point of contact of the wires occur continuously over a period of several seconds in a self-completed manner under constant current supply.

**II. MELTING OF NANOCONTACTS**

Let us consider the electrothermal problem, where two thin wires having the same cross-sectional area  $A$  are in contact with each other with a current  $I$  flowing through them. The temperature at the point of contact governs the melting phenomenon. The contacts melt provided the temperature there reaches the melting point of the material. However, it is not an easy task to determine the temperature at the contact point due to the complex geometry, such as the shapes of asperities, the actual area and location of the contacts, etc. An alternative parameter, which governs the melting phenomenon of the contacts, has been proposed.<sup>22</sup> The parameter  $U$  is described by the following equations:

$$U = u_0 f \quad (1)$$

and

$$u_0 = I \frac{l}{A}, \quad (2)$$

where  $f$  is a function of the geometrical quantities used to represent the difference in thermal boundary conditions between the actual situation and in ideal conditions and  $l$  is the total length of the wire system. The function  $f$  has the value unity in ideal conditions. In ideal conditions, no heat transfer from the wire surface occurs and the temperature of both ends of the wire is kept at room temperature,  $T_0$ . The temperature at the middle of a wire system without a contact,  $T$ , depends on the parameter  $U$  defined in Eq. (1) and is given by

$$T = \frac{1}{8K\sigma} U^2 + T_0, \quad (3)$$

where  $K$  is the heat conductivity and  $\sigma$  the electrical conductivity, respectively. Moreover, for simplicity, if  $\sigma$  is considered to be independent of temperature,  $u_0/\sigma$  corresponds to the voltage between the ends of the wire system.

It was verified from welding and cutting experiments in air that  $U$  governs the melting phenomenon at the contact point between two thin wires and gives the successful welding conditions whether the thin wires are joined or not. The welding of two wires is successful provided that the value of  $U$  is in a specific range, i.e.,  $U_C < U < U_U$ , where  $U_C$  is the critical value of  $U$  for melting of the contact between the wires and  $U_U$  is the upper value of  $U$ . In our previous experiments in air, the value of  $U_C$  was found to be about 70% of  $U_U$ . The reason why the points of contact between two wires melt locally by Joule heating is due to the formation of a specific temperature field in that region. The specific temperature field is formed throughout the contact region due to the higher current density and smaller contact volume and the points in contact melt provided that the temperature at the contacts exceeds the melting point of the material. The wide margin of  $U$  for successful welding gives this welding technique utilizing Joule heating a wide area of applications.

### III. EXPERIMENT

Thin Pt wires with a diameter of  $800 \pm 200$  nm were used in the experiments. The thin wires were Ag-coated, making the overall diameter about  $75 \mu\text{m}$ . This type of wire is known as Wollaston wire.<sup>23</sup> The Ag-coated Pt wires were cut into 10 mm lengths and then the Ag around the tips of the wires was removed by  $\text{HNO}_3$  to expose the Pt wire. Figure 1(a) show a transmission electron microscope (TEM) micrograph of a cross section of the examined Pt wires. No clear grain boundary was observed in the TEM image. The selected area diffraction patterns obtained at any point on the wire showed the same pattern, demonstrating that the wire was of an elongated grain structure.<sup>23</sup> The wires were fixed onto chips containing Cu electrodes and two chips each carrying a Pt wire were placed on piezoelectric manipulators. The piezoelectric manipulators were assembled on the SEM holder for welding the Pt wires in SEM [Fig. 1(b)]. One manipulator moved in the  $z$  direction and the other moved in both  $x$  and  $y$  directions. The SEM was a JSM-6490 (JEOL,

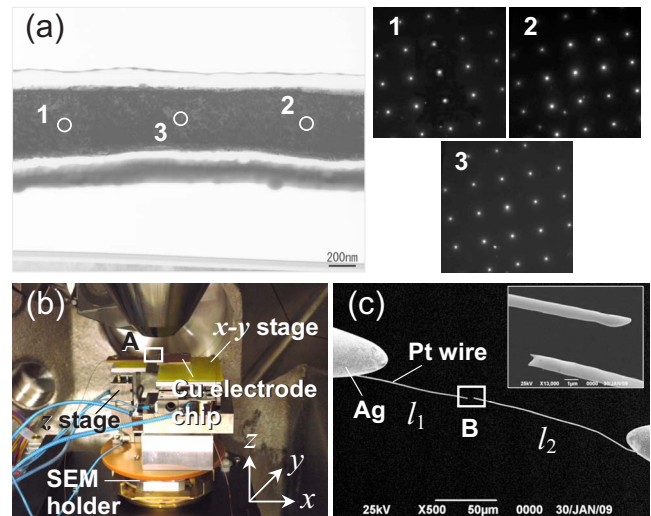


FIG. 1. (Color online) (a) TEM images of the examined Pt thin wire. Selected area diffraction patterns inserted were obtained at the different positions on the wire where the electron-beam direction was parallel to the  $[001]$  of the Pt and those showed that the examined points existed at the same grain. (b) The SEM holder with three-axis piezoelectric manipulators developed for welding two thin wires. (c) The magnification view of A in (b). The Pt wires to be joined are of lengths  $l_1$  and  $l_2$ . Inset shows the details around the tips of the wires. All the experiments were conducted in SEM under the high-vacuum condition.

Tokyo, Japan) and the chamber was kept under high-vacuum conditions of about  $10^{-4}$  Pa.

Using the piezoelectric manipulators, the tips of the wires were brought into contact with each other [Fig. 1(c)]. Here, a small compressive force was applied to the wire system to obtain a stable electrical contact. This was indispensable to keep the wire straight during the melting phase. After contact was confirmed, a constant direct current was applied to the wire system for 20 s. A power source, 6430 (Keithley Instruments, Ohio), placed outside the SEM was used to supply power and measure the voltage and current was carried into the SEM by an electrical feedthrough. The experiments were conducted for combinations of wires with different lengths. The lengths of the exposed Pt wires are denoted by  $l_1$  and  $l_2$ , as shown in Fig. 1(c). After the current supply had been on for 20 s, it was determined by SEM observation whether welding was successful or not. The same process was performed repeatedly with increasing current until the wires were successfully welded. The whole process for welding two Pt wires was conducted *in situ* while under observation in the SEM. The variation of voltage with time was also measured. The same experiments were also conducted in air, where a high-resolution digital microscope was employed and the magnification of the microscope was sufficient for welding experiments.

### IV. RESULTS

Figure 2 shows SEM micrographs during the welding process of two thin wires. Figures 2(a)–2(d) correspond to the

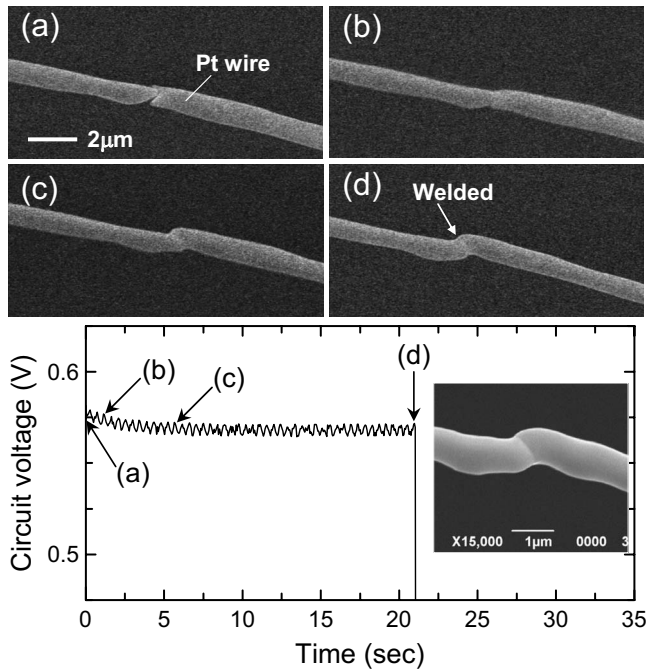


FIG. 2. *In situ* observation of the welding process of two Pt wires. (a) Before current supply. (b)–(d) are the snap shots obtained from the SEM movie at 1, 6, and 21 s after starting the current supply. The corresponding time history for circuit voltage is shown in the lower figure. The applied current was constant at 2.2 mA for 21 s. The welding process that consisted of the melting and solidification at the contact was completed over several seconds after the current supply.

points labeled in the circuit voltage history shown in the lower part of Fig. 2. As reported in our previous experiments, the circuit voltage slightly decreases immediately after the current is supplied.<sup>5</sup> In the SEM micrographs shown in Figs. 2(a) and 2(b), the shape of the parts in contact changed during this period, i.e., several seconds after the supply was switched on. On the other hand, as shown Figs. 2(c) and 2(d), with current still flowing through the wire, from points (c) to (d) the circuit voltage remained constant and no visible change in the contact region was observed. These experimental results show that a changing voltage indicates melting in the contact region, whereas a constant voltage indicates that the contact region has already solidified.

From the SEM observations, the welding mechanism of two thin wires is considered to be as follows. First, the contact region of the wires melts locally by current-induced heating and the contact area increases. The increase in contact area brings about a decrease in circuit resistance and the circuit voltage decreases under the constant current supply. The reduction in Joule heating reduces the temperature in the contact region and the material there solidifies as the temperature falls below the melting point. Note that this welding process is a self-completed mechanism and that melting and solidification in the contact region are achieved within several seconds of turning on the constant current supply.

The results for joining Pt wires are summarized in Table I. Attempts were made to weld two Pt wires of lengths  $l_1$  and  $l_2$  using a current supply of  $I$ . A total of 15 samples (S1–S15)

with different combinations of wires were welded in the SEM, of which 11 samples were successfully welded. Experiments were also conducted in air on five samples (A1–A5) and of these, four combinations were welded. The samples are numbered in order of the total length of the wires. The results are classified into three categories. Successful welding is denoted by S and incomplete welding by N. The symbol M indicates that the welding failed after joining. In this case, the welding was at first successful, but a point in the wire was cut immediately due to higher Joule heating. After the welding was completed, a small shear force was applied in the vicinity of the joint by inclining the wire at about  $5^\circ$ . If the wires separated under this force, the joint was classified as N. The joints were classified after observation with SEM. Note that welds in the SEM were achieved at lower currents than in air (see Table I). In fact, welding was achieved at currents of less than 3 mA, which was insufficient to join the wires in air. This suggests that the temperature reached at the contact point of the wires in the SEM was higher than that in air for the same constant current. This is most likely due to the difference in insulation provided by the vacuum. Heat transfer from the wire surface is restricted under vacuum conditions and this would cause the temperature to rise in the wire system.

## V. DISCUSSION

### A. Thermal function

The difference in the conditions for successful welding between the SEM and air may be due to the difference in thermal boundary conditions between them. In the SEM, the chamber is kept at a high-vacuum level and, therefore, the wire may be affected by greater insulation. The difference in boundary conditions can be described by a function  $f$  and the function is determined from the experiments for cutting thin wires. The current required to cut a wire of length  $l$ , for the case where the temperature of both sides of the wire is constant at  $T_0$  and no heat transfer from the wire surface occurs, can analytically be determined to be

$$(I_C)_0 = \sqrt{(T_M - T_0)8K\sigma} \frac{A}{l}, \quad (4)$$

where  $T_M$  is the melting point of the wire. On the other hand, in the experiments, the current required to cut a wire is described by<sup>22</sup>

$$(I_C)_{\text{exp}} = \sqrt{(T_M - T_0)8K\sigma} \frac{A}{l} \frac{1}{f}. \quad (5)$$

Therefore, the function  $f$  is given by

$$f = \frac{(I_C)_0}{(I_C)_{\text{exp}}}. \quad (6)$$

To determine  $f$  in the SEM and in air, cutting experiments for the Pt wires were conducted. As well as the thin Pt wires, cone-shaped Ag probes were also attached to the Cu electrode chips and these were used to locally supply current to a segment of the Pt wires [see Fig. 3(a)]. The length of the Pt

TABLE I. Results of welding experiments.

Sample No. <sup>a</sup>	Symbol <sup>b</sup>	$l_1$ ( $\mu\text{m}$ )	$l_2$ ( $\mu\text{m}$ )	$l^c$ ( $\mu\text{m}$ )	$I$ (mA)
S1	S	202.8	186.6	389.4	1.0
S2	S	289.1	66.4	355.5	1.0
S3	S	104.2	179.4	283.6	1.7
S4	S	130.7	110.8	241.5	2.0
S5	S	96.0	143.0	239.0	2.2
S6	S	75.1	126.1	201.2	2.5
S7	S	35.7	151.5	187.2	1.7
S8	M	66.4	114.6	181.0	2.9
S9	S	69.2	86.1	155.3	2.8
S10	N	70.5	80.3	150.8	2.2
	S				2.6
S11	N	53.8	84.5	138.3	2.2
	S				2.4
S12	N	62.5	74.5	137.0	2.0
	M				3.5
S13	M	48.2	74.5	122.7	3.5
S14	S	50.1	57.3	107.4	4.5
S15	M	57.1	33.1	90.2	5.3
A1	N	243.0	53.9	296.9	3.0
	S				3.5
A2	N	141.7	104.3	246.0	3.0
	S				4.5
A3	N	108.1	75.2	183.3	3.2
	S				4.0
A4	N	66.9	56.8	123.7	4.1
	S				5.6
A5	M	46.6	61.9	108.5	6.5

<sup>a</sup>Experiments were conducted in a SEM (S1–S15) and in air (A1–A5).

<sup>b</sup>S indicates successful welding and N incomplete welding. The case of a joint that was cut during the current supply due to higher Joule heating is classified as M.

<sup>c</sup>The diameter of all wires was 800 nm and  $l$  is given by  $l_1+l_2$ .

wire with current flowing, i.e., the distance between the root of the wire and the contact point of the Ag probe,  $l$ , was 50, 100, 200, 300, or 400  $\mu\text{m}$ . A small force, which was needed to shear the molten part of the wire and thus cut the wire, was applied by bending the wire with the Ag probe. Current was supplied to the wire system for 20 s. If the wire remained intact, the supply was stopped. The current was increased by 0.1 mA and the experiment repeated. This process was repeated until the wire was cut [Fig. 3(b)]. For all values of  $l$  examined, the wires were cut at the center. Figure 3(c) shows the current required to cut wires in the SEM and in air for various values of  $l$ . The current decreases as  $l$  increases and the currents required for cutting the wire in the SEM are lower than those in air.

Figure 3(d) shows the relationship between  $f$  and  $d/l$  for the SEM and air environments. Here we assume that the melting point of the Pt wire is  $T_M=2042$  K (Ref. 24) and that  $T_0=293$  K. Because the value of  $d$  is constant in the present study, smaller values of  $d/l$  indicate longer  $l$ . By

nonlinear fitting, we obtained the following  $f$  for each environment:

$$f_1 = -29.1 \times 10^2 \left(\frac{d}{l}\right)^2 + 90.7 \frac{d}{l} + 2.9 \quad (7)$$

for the SEM environment and

$$f_2 = -126 \times 10^2 \left(\frac{d}{l}\right)^2 + 407 \frac{d}{l} \quad (8)$$

for the air environment. The function  $f_2$  is the modified function and a similar function has been reported previously.<sup>22</sup> Here, we performed similar experiments for different values of  $l$  and expanded the range of  $d/l$ . The present functions of  $f_1$  and  $f_2$  are valid for  $d/l < 0.016$ .

Values of  $f$  greater than unity indicate that the temperature at the middle of the wire in a realistic situation is higher than that for the ideal conditions considered, in which there is no heat loss from the wire, and this is due to the difference in



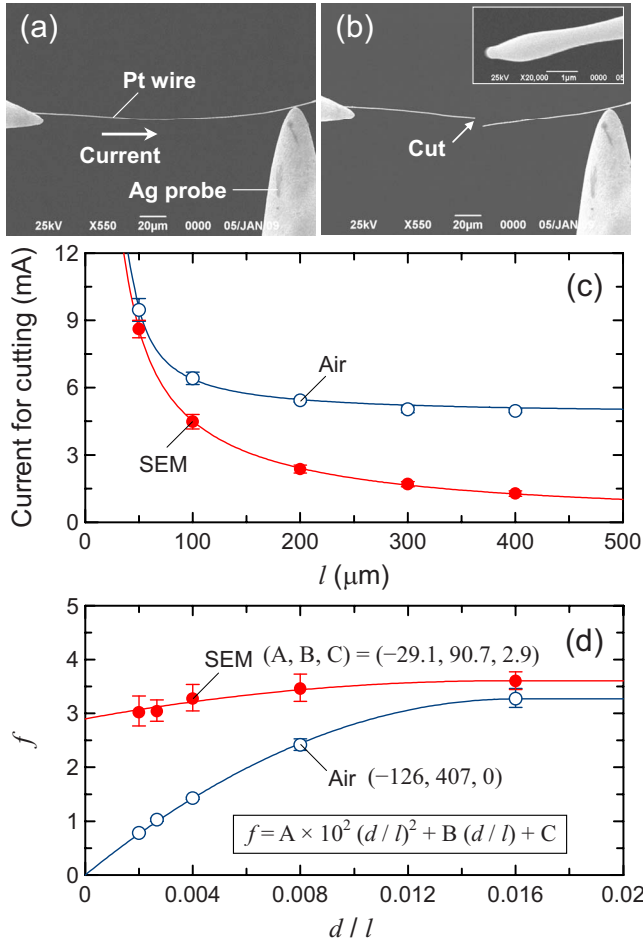


FIG. 3. (Color online) SEM micrographs obtained in the cutting experiment in the case of  $l=200\ \mu\text{m}$  (a) before and (b) after a current supply of  $I=2.7\ \text{mA}$ . Inserted micrograph in (b) shows the swelled tip of the cut wire. (c) Current required for cutting thin Pt wires in SEM and air for various wire lengths. (d) The relationships between  $f$  and  $d/l$  for SEM and air environments obtained from the cutting experiments.

temperature at the ends of the wire. Although the temperature of both ends of the wire was considered to be constant at  $T_0$  for the ideal conditions, it is higher than  $T_0$  in a realistic situation. On the other hand, if the temperature at the middle of the wire in a realistic situation becomes less than that of the ideal conditions,  $f$  becomes less than unity. This situation is brought about by the difference in heat loss from the wire surface. In a realistic situation, heat loss occurs from the wire surface and this becomes significant for longer wires. On the other hand, there is no heat loss from the wire surface for the ideal conditions.

In the examined range of  $d/l$ ,  $f_1$  is larger than  $f_2$ . This indicates that the temperature of the wire easily increases in the SEM compared to in air. This is due to the difference in heat loss from the wire surface and the significant effect of insulation in the SEM. Actually, this tendency was more remarkable for longer wires (smaller  $d/l$ ). The larger surface area of longer wires gave greater heat exchange between the wire and the environment due to the larger surface-to-volume ratio. Needless to say, if the temperature distribution in the

wire changes, heat conduction in the wire also changes. As a result, the temperature at both ends of the wire would change. For shorter wires (larger  $d/l$ ),  $f_1$  approaches  $f_2$ . This is because heat loss from the wire surface is ineffective for shorter wires, which have insufficient surface area, and the difference between the environments is minimal. In both SEM and air, the value of  $f$  approaches 3.5 for shorter wires. This value of  $f$  depends on the balance of heat conduction in the wire and indicates that the temperature at each end of the wire is greater than  $T_0$ .

Let us consider the difference in the limit of  $(I_C)_{\text{exp}}$  for longer wires. From Eqs. (5) and (7), the value of  $(I_C)_{\text{exp}}$  for longer wires in the SEM is given by

$$\lim_{l \rightarrow \infty} (I_C)_{\text{exp}} = \lim_{l \rightarrow \infty} A \sqrt{(T_M - T_0) 8K\sigma} \times \frac{1}{-29.1 \times 10^2 \frac{d^2}{l} + 90.7d + 2.9l} \rightarrow 0. \quad (9)$$

In the case of the SEM, a very small current, i.e., almost zero, is enough for cutting extremely long wires. This is due to the greater insulation in the SEM. On the other hand, from Eqs. (5) and (8), the value of  $(I_C)_{\text{exp}}$  for longer wires in air is

$$\lim_{l \rightarrow \infty} (I_C)_{\text{exp}} = \lim_{l \rightarrow \infty} A \sqrt{(T_M - T_0) 8K\sigma} \times \frac{1}{-126 \times 10^2 \frac{d^2}{l} + 407d} \rightarrow 4.8\ \text{mA}. \quad (10)$$

In the limit of  $f_2$  for longer wire, a critical current for cutting the wire exists. Because of the heat loss from the wire surface, the temperature at the middle of the wire never reaches the melting point unless the current is greater than this critical value. In this experiment, the critical value for cutting the wire is about 4.8 mA and wires of any length would not be cut under 4.8 mA.

## B. Condition for joining Pt wires

Figures 4(a) and 4(b) display the relationships between the values of  $U$  and  $d/l$  for the welding and cutting experiments done in the SEM (a) and in air (b), respectively. The parameter  $U$  defined by Eq. (1) corresponds to the temperature at the middle of the wire system without a contact and it governs the melting phenomenon at the nanocontact between two thin wires. Two wires were found to be successfully welded provided that the value of  $U$  is in a specific range, i.e.,  $U_C < U < U_U$ . The values of  $U_U$  and  $U_C$  were determined for thin Pt wires in air in our previous study.<sup>22</sup>  $U_U$  was 3.1 MA/m and  $U_C$  was found to be about 70% of  $U_U$  ( $=2.2\ \text{MA/m}$ ).

The values of  $U$  for successful welding are found to be in a specific range for both SEM [Fig. 4(a)] and air [Fig. 4(b)] environments and the welding conditions defined by  $U$  were found to be independent of environment. Because the difference in thermal boundary conditions was calibrated in  $U$  by  $f$ , the difference in welding current between the SEM and air

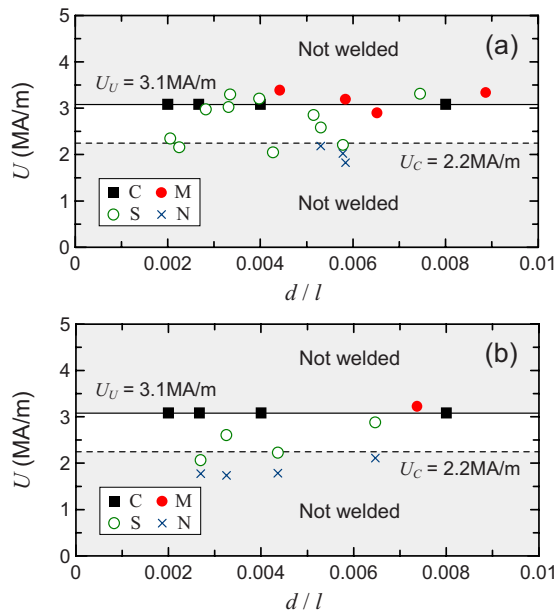


FIG. 4. (Color online) The relationship between the values of  $U$  for successful welding and  $d/l$  for the welding experiments in (a) SEM and (b) air. Here, the open circles show successful welding (S) and the crosses mark incomplete welding (not joined) (N). Solid circles also show welding where the wires were immediately cut after joining due to higher Joule heating (M). The data for the cutting experiments are plotted with solid squares (C).

environments was due to the difference in the thermal boundary conditions, e.g., the heat loss from the wire surface and the temperature at both ends of the wires. In other words, the specific temperature distribution at the nanocontact between two thin wires, that gives roughly 70% higher temperature than that at the center of a wire system without a contact,<sup>25</sup> is preserved independently of the thermal boundary conditions of the wires. This finding is important for

understanding welding of thin wires under various environments and thermal boundary conditions. The current to achieve successful welding can be decided provided that  $f$  for the environment is known. Moreover, longer thin wires may possibly be fabricated by repeatedly welding wires. In this case, the current should be decided by considering the total length of the wires to be joined and the environmental situation.

## VI. CONCLUSIONS

Thin Pt wires with diameters of about 800 nm were successfully welded by current-induced heating in a scanning electron microscope and in air. It was observed from *in situ* observations of the welding process that melting and solidification occur continuously under a constant current supply and that the process is self-completed within several seconds. The current required to weld two wires in the SEM was much less than that in air. This was due to the difference in pressure between the environments. Due to the insulation under vacuum conditions, the temperature of the wire is easily raised by Joule heating. The influence of the thermal boundary conditions on the welding process brought about by the geometrical features of the thin wires, i.e., wide surface area compared to diameter, was substantial. The difference in the thermal boundary conditions between the microscope and air were evaluated by a thermal function and welding conditions that are independent of the surrounding environment were found.

## ACKNOWLEDGMENTS

The authors would like to acknowledge M. Saka for his valuable discussions throughout this work. This work was supported by Grant-in-Aid for Young Scientists (A) Grant No. 21686012 and by Grant-in-Aid for Scientific Research (S) Grant No. 18106003.

\*Corresponding author; tohmyoh@ism.mech.tohoku.ac.jp

<sup>1</sup>Y. Wu and P. Yang, *Adv. Mater.* **13**, 520 (2001).

<sup>2</sup>S. Tan, Z. Tang, X. Liang, and N. A. Kotov, *Nano Lett.* **4**, 1637 (2004).

<sup>3</sup>S. Xu, M. Tian, J. Wang, J. Xu, J. M. Redwing, and M. H. W. Chan, *Small* **1**, 1221 (2005).

<sup>4</sup>X. Li, H. Gao, C. J. Murphy, and K. K. Caswell, *Nano Lett.* **3**, 1495 (2003).

<sup>5</sup>H. Tohmyoh, T. Imaizumi, H. Hayashi, and M. Saka, *Scr. Mater.* **57**, 953 (2007).

<sup>6</sup>Y. Peng, T. Cullis, and B. Inkson, *Nano Lett.* **9**, 91 (2009).

<sup>7</sup>S. H. Tsai, C. T. Shiu, W. J. Jong, and H. C. Shih, *Carbon* **38**, 1899 (2000).

<sup>8</sup>H. Hirayama, Y. Kawamoto, Y. Ohsima, and K. Takayanagi, *Appl. Phys. Lett.* **79**, 1169 (2001).

<sup>9</sup>A. V. Krashennnikov, K. Nordlund, J. Keinonen, and F. Banhart, *Phys. Rev. B* **66**, 245403 (2002).

<sup>10</sup>C. Chen, L. Yan, E. S.-W. Kong, and Y. Zhang, *Nanotechnology*

**17**, 2192 (2006).

<sup>11</sup>F. Bussolotti, L. D'Ortenzi, V. Grossi, L. Lozzi, S. Santucci, and M. Passacantando, *Phys. Rev. B* **76**, 125415 (2007).

<sup>12</sup>C. Jin, K. Suenaga, and S. Iijima, *Nat. Nanotechnol.* **3**, 17 (2008).

<sup>13</sup>J. Huang and R. B. Kaner, *Nature Mater.* **3**, 783 (2004).

<sup>14</sup>S. J. Kim and D.-J. Jang, *Appl. Phys. Lett.* **86**, 033112 (2005).

<sup>15</sup>J. A. Riley, *Science* **109**, 281 (1949).

<sup>16</sup>M. C. Salvadori, A. R. Vaz, F. S. Teixeira, M. Cattani, and I. G. Brown, *Appl. Phys. Lett.* **88**, 133106 (2006).

<sup>17</sup>J. Wang, M. S. Gudiksen, X. Duan, Y. Cui, and C. M. Lieber, *Science* **293**, 1455 (2001).

<sup>18</sup>D. Li, Y. Wu, P. Kim, L. Shi, P. Yang, and A. Majumdar, *Appl. Phys. Lett.* **83**, 2934 (2003).

<sup>19</sup>A. N. Goldstein, C. M. Echer, and A. P. Alivisatos, *Science* **256**, 1425 (1992).

<sup>20</sup>J. Wang, X. Chen, G. Wang, B. Wang, W. Lu, and J. Zhao, *Phys.*

Rev. B **66**, 085408 (2002).

<sup>21</sup>K. Dick, T. Dhanasekaran, Z. Zhang, and D. Meisel, J. Am. Chem. Soc. **124**, 2312 (2002).

<sup>22</sup>H. Tohmyoh, J. Appl. Phys. **105**, 014907 (2009).

<sup>23</sup>A. C. Sacharoff and R. M. Westervelt, Phys. Rev. B **29**, 6411 (1984).

<sup>24</sup>Z. L. Wang, J. M. Petroski, T. C. Green, and M. A. El-Sayed, J. Phys. Chem. B **102**, 6145 (1998).

<sup>25</sup>Inserting  $U=2.2$  MA/m ( $U_C$ ) into Eq. (3), we get  $T=1180$  K. On the other hand, because the contact region of two wires melts under this condition, the temperature at the contacts is considered to be  $T_M=2042$  K. The ratio  $T_M/T$  is about 1.7.